Biomaterials 45 (2015) 46–55

Contents lists available at ScienceDirect

Biomaterials

journal homepage: www.elsevier.com/locate/biomaterials

Multi-level characterization of human femoral cortices and their underlying osteocyte network reveal trends in quality of young, aged, osteoporotic and antiresorptive-treated bone

Petar Milovanovic [a, b], Elizabeth A. Zimmermann [a], Christoph Riedel [a], Annika vom Scheidt [a], Lydia Herzog [a], Matthias Krause [a], Danijela Djonic [b], Marija Djuric [b], Klaus Püschel [c], Michael Amling [a], Robert O. Ritchie [d, e], Björn Busse [a, e, *]

[a] Department of Osteology and Biomechanics, University Medical Center Hamburg-Eppendorf, Lottestrasse 59, 22529 Hamburg, Germany
[b] Laboratory for Anthropology, Institute of Anatomy, Faculty of Medicine, University of Belgrade, Dr Subotica 4/2, 11000 Belgrade, Serbia
[c] Department of Forensic Medicine, University Medical Center Hamburg-Eppendorf, Butenfeld 34, 22529 Hamburg, Germany
[d] Department of Materials Science and Engineering, University of California, Berkeley, USA
[e] Materials Sciences Division, Lawrence Berkeley National Laboratory, Berkeley CA 94720, USA

ARTICLE INFO

Article history:
Received 1 September 2014
Accepted 20 December 2014
Available online

Keywords:
Mechanical properties
Fracture mechanism
Biomineralization
Microstructure
Osteoporosis
Bone

ABSTRACT

Characterization of bone's hierarchical structure in aging, disease and treatment conditions is imperative to understand the architectural and compositional modifications to the material and its mechanical integrity. Here, cortical bone sections from 30 female proximal femurs – a frequent fracture site – were rigorously assessed to characterize the osteocyte lacunar network, osteon density and patterns of bone matrix mineralization by backscatter-electron imaging and Fourier-transform infrared spectroscopy in relation to mechanical properties obtained by reference-point indentation. We show that young, healthy bone revealed the highest resistance to mechanical loading (indentation) along with higher mineralization and preserved osteocyte-lacunar characteristics. In contrast, aging and osteoporosis significantly alter bone material properties, where impairment of the osteocyte-lacunar network was evident through accumulation of hypermineralized osteocyte lacunae with aging and even more in osteoporosis, highlighting increased osteocyte apoptosis and reduced mechanical competence. But antiresorptive treatment led to fewer mineralized lacunae and fewer but larger osteons signifying rejuvenated bone. In summary, multiple structural and compositional changes to the bone material were identified leading to decay or maintenance of bone quality in disease, health and treatment conditions. Clearly, antiresorptive treatment reflected favorable effects on the multifunctional osteocytic cells that are a prerequisite for bone's structural, metabolic and mechanosensory integrity.

1. Introduction

Bone is a complex hierarchically organized material consisting of osseous cells and a nano-composite structure composed of collagen and mineral [1,2]. Osteocytes are the most frequent occurring osseous cell type in the skeleton, which are strategically distributed throughout the entire mineralized bone. Therefore, they play a key role in the mechanosensitive behavior of bone [3] by detecting mechanical stimulation and orchestrating signal transmission between bone cells involved in bone repair and renewal. Such chemically and/or mechanically triggered responses through either intracellular calcium transients [4] or the release of nitric oxide and prostaglandin E2 [3,5–7] are critical to bone health and bone remodeling. Osteocytes reside in special cavities within the bone matrix called osteocyte lacunae and are separated from direct contact with the mineralized bone matrix through a thin layer of unmineralized tissue [8,9]. Although much of the relationship between the cell and the lacunar space is still unknown, osteocytes are believed to actively modify their surrounding environment [10,11], and cellular viability is essential for maintaining the lacunar space [12,13]. The osteocytes' characteristics are thought to

* Corresponding author. Emmy Noether Research Group, c/o Department of Osteology and Biomechanics, University Medical Center Hamburg-Eppendorf, Lottestr. 59, 22529 Hamburg, Germany. Tel.: +49 40 7410 56687.
E-mail address: b.busse@uke.uni-hamburg.de (B. Busse).

http://dx.doi.org/10.1016/j.biomaterials.2014.12.024
0142-9612/

describe the bone's matrix potential mechanosensory abilities, adaptative capacity and possibly the quality of the perilacunar tissue [2,12,14–18]. However, the death of an osteocyte within the lacuna is associated with a phenomenon termed 'micropetrosis', where the lacuna becomes completely mineralized [19]. Mineralized lacunae are thought to represent osteocytes' "fossils" as the apoptotic remnants of osteocytes have been found within the mineralized material [13]. Due to the possible negative impact of mineralized lacunae on bone health [12,20], we hypothesize that the occurrence of mineralized lacunae serves as a marker for *bone quality*. *Bone quality* is a critical aspect in maintaining bone mechanical competence as it describes the totality of features and characteristics that influence a bone's ability to resist fractures [21]. Specifically, bone quality encompasses both the composition and structure of bone through the degree of mineralization, the type of cross-linking, collagen characteristics, the presence of microdamage and non-collagenous proteins, as well as architecture/geometry patterns [1,22,23].

Previous studies have observed that the mineralization of osteocyte lacunae can be attributed to aging and the existence of skeletal diseases [12,20,24]. Thus, changes in the mineralization of osteocyte lacunae may indeed reflect bone quality and the risk of fracture in humans. However, the trends in the number and degree of mineralized lacunae and the corresponding effect on bone remodeling have not been comprehensively studied. In particular, it is of interest if age- and disease-dependent mineral occlusions of osteocyte lacunae may be prevented by bisphosphonate (BP) treatment. Indeed, anti-resorptive treatment was found to increase areal bone mineral density and decrease fracture risk [25–28]. However, associated side effects in the form of new atypical fractures related to bisphosphonate-treatment are reported as well [29,30]. Although *in vitro* and animal model studies suggested that bisphosphonates promote osteoblasts viability and express anti-apoptotic effects on osteocytes [31–33], histological findings on dogs' ribs rather showed decreased osteocyte lacunar density following long-term alendronate treatment [34]. Therefore, bisphosphonates' specific species- and site-related modes of action deserve additional attention to unravel corresponding wide-ranging effects taking place on several bone tissue hierarchical levels.

In the present study, we quantify the density and distribution of mineralized lacunae within the femoral cortical bone in young, aged, osteoporotic and alendronate-treated individuals. In addition to a rigorous assessment of osteocyte lacunar characteristics, we analyzed the bone matrix's composition and its mechanical competence in the four groups to provide a better understanding of the bone quality and osteocytes' contribution to bone health with special regard to bone remodeling characteristics in health, disease and bisphosphonate-treatment stage. The bone's composition and mechanical properties are important to understand the mechanisms that lead to fracture in human bone, teeth and other biological materials, and for providing insights on the prerequisites for designing and using new bone replacement materials and/or pharmacologic treatment options to cure bone-related diseases.

2. Materials and methods

The bone specimens used in this study were acquired during autopsy at the Department of Forensic Medicine, University Medical Center Hamburg-Eppendorf, Hamburg, Germany, from 30 female individuals. Based on autopsy reports and clinical histories, the individuals were divided into four study groups:

1. Young female individuals without skeletal diseases/fractures (age 31.4 ± 9.5 years, n = 5)
2. Aged female individuals without skeletal diseases/fractures (age 83.7 ± 5.9 years, n = 7)
3. Female individuals with untreated osteoporosis (age 82.5 ± 5.5 years, n = 9)
4. Female individuals with osteoporosis who received bisphosphonate treatment (age 80.5 ± 7.2 years, n = 9).

These individuals did not suffer from cancer, renal diseases, primary hyperparathyroidism, or Paget's disease and did not show any other signs or symptoms of bone diseases apart from postmenopausal osteoporosis in the appropriate groups. The treated osteoporosis group received the third-generation bisphosphonate alendronate at either 10 mg per day or 70 mg per week during 6 ± 1.6 years.

The study was approved by the Ethics Committee of the Hamburg Chamber of Physicians (PV3486).

2.1. Specimen preparation

A complete horizontal cross-section of the proximal diaphysis of each femur (from all four groups of patients), as well as cross-sections of distal radius, iliac crest and the L5 vertebral body (from osteoporosis and alendronate-treated patients) were cut using a diamond belt saw (Exakt, Norderstedt, Germany) and fixed in formalin (3.5%), as reported previously [35]. The slice thickness in all specimens was 4 mm. The undecalcified specimens were dehydrated by means of an ascending ethanol series (70%, 80%, 2 × 96%, 3 × 100%) and further infiltrated with a plastic embedding medium (Technovit 7200; Heraeus/Kulzer, Wehrheim/Ts., Germany). The infiltration was performed in steps with the following volumetric ethanol/Technovit-ratios: 70:30; 50:50; 30:70; 0:100. Finally, Technovit with benzoyl-peroxide was used to continue the infiltration process for another 10 days. Ground tissue specimens were made based on Donath's grinding technique [35,36]. After the grinding and polishing processes, the specimens were carbon coated and prepared for scanning electron microscopy.

2.2. Scanning electron microscopy (SEM): evaluation of osteocyte lacunae

The femur specimens were mounted in a scanning electron microscope (LEO 435 VP; LEO Electron Microscopy Ltd., Cambridge, England) with a backscattered electron detector (Type 202, K.E. Developments Ltd., Cambridge, England). The microscope was operated in backscattered electron mode at 20 keV and a constant working distance, while the images were acquired with 100x magnification. The following parameters were evaluated in the femur samples: number of mineralized lacunae per bone area and total number of lacunae per bone area. Mineralized lacunae were defined following the criteria from backscattered electron imaging [12,20]. The bone area was evaluated with ImageJ software (ImageJ, 1.45q, National Institutes of Health, USA – imagej.nih.gov/ij/) using the BoneJ plugin for bone volume fraction [37].

To assess the spatial distribution of osteocyte lacunae, the femoral cortical cross-section was divided into four regions (i.e., medial, lateral, ventral, and dorsal), and each region was then subdivided into periosteal and endosteal compartments, as in previous studies [12,38]. In each of the four regions of the femoral cross-sections (i.e., medial, lateral, ventral and dorsal), a minimum of two representative images per compartment (each approximately 1 mm^2) were analyzed.

The number of Haversian systems per bone area was evaluated on the same images that were used to quantify the osteocyte lacunae. Thus, the density of osteons provides an overview (history) of the number of remodeling events [38].

2.3. Bone mineral density distribution analysis (BMDD) using quantitative backscattered electron imaging (qBEI)

We performed quantitative backscattered electron imaging (qBEI) to evaluate the bone mineral density distribution (BMDD) in cross-sections from the femora, radii, iliac crests and vertebral L5 bodies in accordance with previous studies [2,39–43]. The scanning electron microscope was operated in backscatter mode at 20 keV and 680 pA with a constant working distance of 20 mm. The beam current was controlled by use of a Faraday cup (MAC Consultants Ltd., England), and all parameters were maintained stable during imaging. The gray level was calibrated with a standard of known density, as explained in more details in previous studies, such that gray level had a linear relationship with the calcium concentration [41]. The qBEI measurements were performed on images with 50x magnification. Using a custom Matlab routine, the following parameters were automatically evaluated: mean calcium concentration (mean Ca, wt%), most frequent calcium concentration (peak Ca, wt%), standard deviation of the calcium distribution curve showing the degree of heterogeneity of BMDD distribution (width Ca, wt%), percentage of bone area that is mineralized below the 5th percentile of the reference range of the young group (Ca low, % bone area) and percentage of bone area containing Ca concentration above the 95th percentile of the reference range of the young group (Ca high, % bone area). In each individual, two images per compartment per region (each approximately 4 mm^2 in size) were considered for the qBEI evaluations.

2.4. Fourier transform infrared spectroscopy (FTIR)

To assess the quality of the bone matrix, Fourier transform infrared (FTIR) spectroscopy was performed within the medial, lateral, ventral, and dorsal regions of each femur sample. The FTIR spectra were acquired with a Universal ATR sampling accessory connected to a Frontier FTIR spectrometer (Perkin Elmer, Waltham, MA, USA). Spectra were acquired over a spectral range of 570–4000 cm^{-1} at a spectral

resolution of 4 cm^{-1} and 128 scans. Spectra were analyzed using a custom program in Matlab (MathWorks, Natick, MA, USA), where each sample was baseline corrected from 1850 to 1950 cm^{-1}. The mineral to matrix ratio was calculated by taking the area ratio of the phosphate peak at 890–1180 cm^{-1} to the amide I peak at 1600–1710 cm^{-1}. The carbonate to phosphate ratio was calculated by taking the area ratio of the carbonate peak at 850–890 cm^{-1} to the phosphate peak at 890–1180 cm^{-1}.

2.5. Reference point indentation (RPI)

The polished femoral cross-sections were mounted on BioDent Hfc instrument for reference point indentation (Active Life Scientific Inc., Santa Barbara, CA, USA). Reference point indentation (RPI) is a microindentation method used for mechanical probing of mineralized tissues [44], which has potential for clinical application [45,46]. Here, the RPI measurements were performed using a probe (BP2 probe: Active Life Scientific Inc., Santa Barbara, CA, USA) consisting of a *reference probe* that rests on the bone surface (initial touchdown) and a *test probe* which indents the bone when the load is applied [44]. The test probe is 90° conospherical with less than 5 μm radius point. Basically, the RPI technique encompasses successive indentation cycles, where with each cycle the test probe progresses deeper into the bone tissue. Unlike some previous studies that performed RPI on periosteal bone surfaces [45–47], in this study the indents were made on femoral cross-sections in order to correlate the mechanical characteristics with simultaneously acquired structural and compositional properties. In each individual, a minimum of three measurements per compartment per region were acquired. All the indents were retrospectively imaged via electron microscopy to ensure that only the bone matrix was subject to indentation, rather than voids, pores or bone marrow regions. Here, the RPI was performed with an indentation frequency of 2 Hz, an applied force of 6 N and 10 successive indentations (indentation cycles) per measurement. Based on the load–displacement curves recorded by the Biodent software, the following parameters were measured: first cycle indentation distance (ID 1, μm) – the indentation depth after the first indentation cycle (i.e., the distance between the reference probe and test probe after the first indentation cycle), total indentation distance (TID, μm) – the distance between the reference probe and test probe after the last indentation cycle (i.e., maximum indentation distance after the last cycle), indentation distance increase (IDI, μm) which is the increase in indentation distance between the first and last cycle, and average energy dissipated (ED, μJ) representing the average area under the load–displacement curve. Although precise mechanical meaning of all RPI parameters is not yet fully understood, recent studies showed strong correlation between RPI and traditional mechanical testing methods; in this context, first cycle indentation distance is usually regarded as an inverse estimate of microhardness, while dissipated energy and indentation distance increase may reflect bone material's toughness [46,48,49].

2.6. Statistical analysis

The normal distribution of data was tested using the Kolmogorov–Smirnov test. To address whether the investigated bone properties differ between the

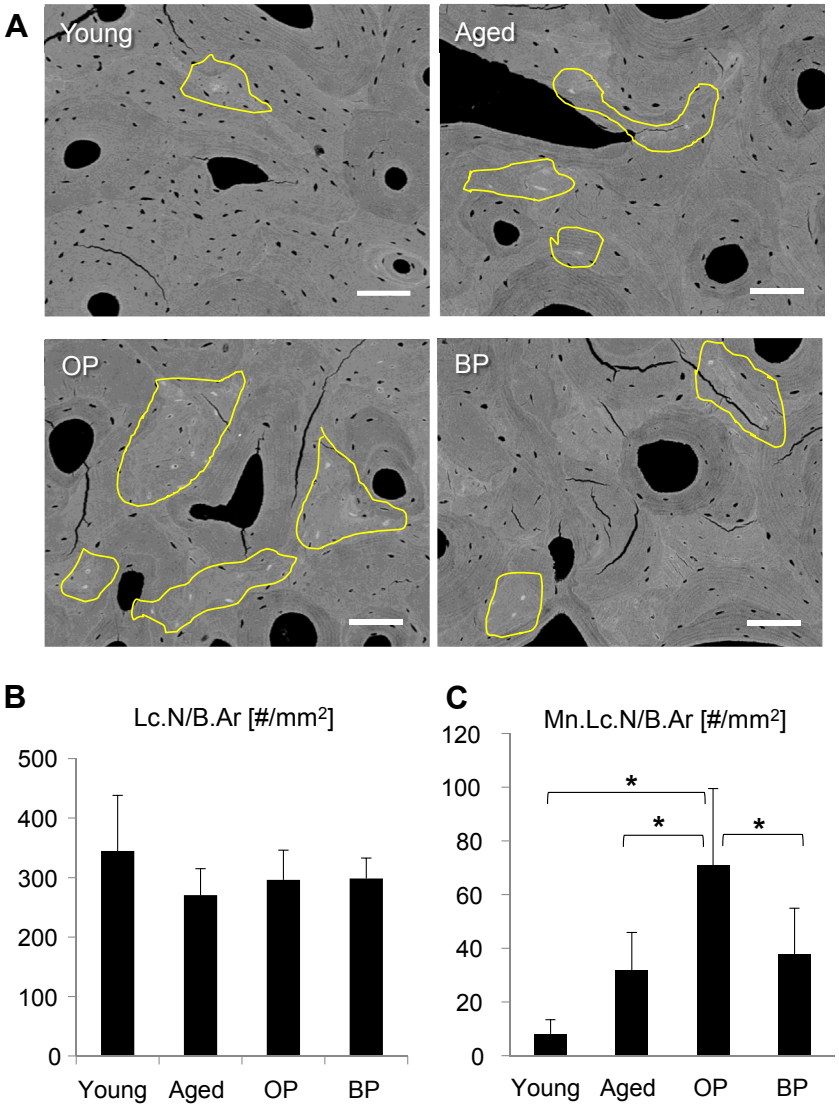

Fig. 1. Osteocyte lacunar characteristics of the femoral cortical bone. The analyses refer to specimens from young, aged, untreated osteoporosis (OP) and bisphosphonate-treated (BP) women. (A) Backscattered electron images reveal osteocyte lacunar characteristics. Note differential occurrence of hypermineralized osteocyte lacunae, especially in interstitial bone (encircled by yellow lines) (Scale bar 100 μm). (B) Inter-group differences in lacunar number per bone area. (C) Inter-group differences in mineralized lacunae number per bone area. (* - $p < 0.05$). Error bars represent SD. (For interpretation of the references to colour in this figure legend, the reader is referred to the web version of this article.)

groups, as well as among various regions, the analysis of variance (ANOVA) for repeated measurements was performed. As the difference between regions belonging to the same individual was evaluated, the region was defined as "within-subject factor", while differences between the groups were analyzed after setting the group as "between-subject factor". Interaction of group and region was also chosen to check whether the evaluated parameters showed similar or different region-dependence among different groups. The post-hoc procedures to assess the differences in evaluated parameters between individual groups, as well as regions were conducted under Bonferroni correction for multiple comparisons. Pearson's correlation coefficient was used to test the relationship between various parameters.

All analyses were performed using Statistical Package for the Social Sciences (SPSS) version 15.0, and the level of significance considered to be statistically significant was 0.05.

3. Results

3.1. Inter-group differences in osteocyte lacunar numbers in the femoral cortex

Backscattered electron imaging allowed us to evaluate the number and distribution of osteocyte lacunae, as well as their composition in the femoral cortical bone. Two different types of lacunae were observed: lacunae that appear black and those that are filled with a bright contrast. The black lacunae most likely signify the presence of a living osteocyte, while the filled or partially filled lacunae mostly observed in interstitial bone regions

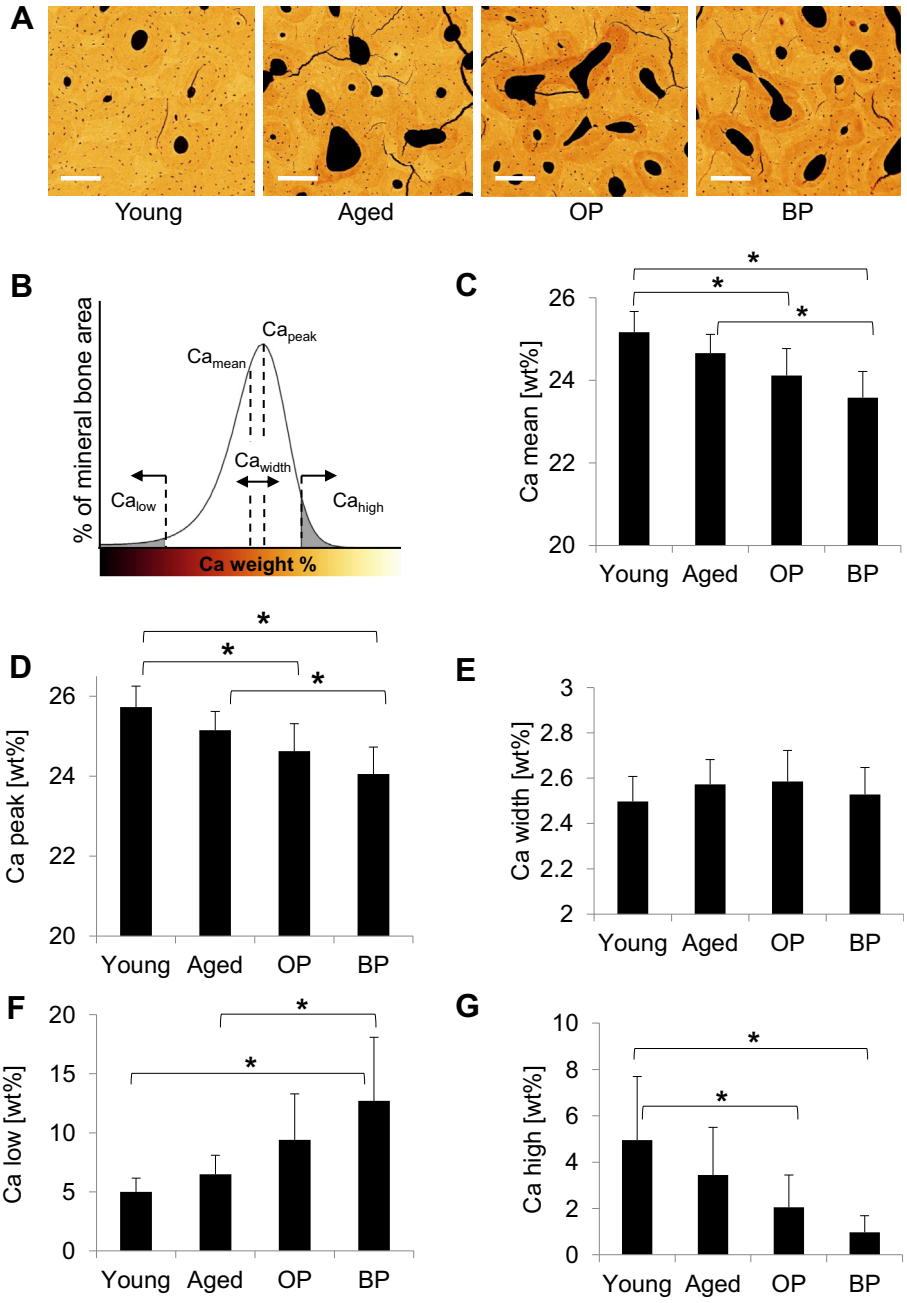

Fig. 2. Bone mineral density distribution as revealed by quantitative backscattered-electron imaging of the femoral cortical bone. (A) Representative backscattered electron images from young, aged, untreated osteoporosis (OP) and bisphosphonate-treated (BP) women (Scale bar 200 μm). (B) Schematic representation of the quantitative parameters obtained by the qBEI method. (C) Inter-group differences in mean Ca content, (D) peak Ca content, (E) homogeneity of mineralization distribution, i.e. Ca width, (F) low Ca and (G) high Ca values. (* – $p < 0.05$). Error bars indicate SD.

(Fig. 1A) contain calcium phosphate deposits. Overall the total lacunar number per bone area was not significantly different between the study groups (Fig. 1B). However, trends in the number of mineralized lacunae were apparent with the young cortex having the lowest number of hypermineralized lacunae per bone area and the osteoporotic cortex containing a significantly higher occurrence of micropetrotic occlusions in comparison to young, healthy aged and bisphosphonate-treated osteoporotic cases (Fig. 1A, C).

3.2. Bone matrix mineralization in the femoral cortex via qBEI and FTIR

Quantitative backscattered electron imaging was also used to evaluate the bone mineral density distribution in the study groups (Fig. 2A–G). QBEI imaging of the femoral cortical bone revealed significant inter-group differences in Ca mean and Ca peak ($p < 0.001$) (Fig. 2C,D). Post-hoc tests showed that bisphosphonate-treated cases had a significantly lower mineral density distribution as measured through the Ca mean and Ca peak than the young and aged cases, while the young cases had a higher mineral density distribution than osteoporotic cases. Similarly, Ca low was significantly dependent on the group with the bisphosphonate-treated individuals showing significantly higher Ca low values than the young and aged individuals (Fig. 2F). Ca high was significantly lower in osteoporosis and bisphosphonate-treated cortices than in the young group (Fig. 2G). Thus, high spatial resolution qBEI measurements indicate an overall trend towards a higher femoral mineral density distribution in young cases and a lower mineral density distribution in osteoporosis and bisphosphonate-treated cases.

The FTIR results (Fig. 3A, B) support the qBEI data, where the mineral-to-matrix ratio correlated with the qBEI-derived Ca mean ($r = 0.585$, $p = 0.001$) and Ca peak values ($r = 0.492$, $p = 0.008$). ANOVA showed significant inter-group differences in the mineral-to-matrix ratio (Fig. 3A), with the highest values observed in young femoral cortices and the lowest in bisphosphonate-treated cases. Post-hoc tests revealed that the young cortices showed a significantly higher mineral-to-matrix ratio than the osteoporosis and bisphosphonate-treated groups. Although not significant, the carbonate-to-phosphate ratio (Fig. 3B) showed a trend of lower values in osteoporosis and bisphosphonate-treated cases and correlated positively with Ca mean ($r = 0.493$, $p = 0.008$) and Ca peak ($r = 0.479$, $p = 0.01$), as well as with mineral-to-matrix ratio ($r = 0.486$, $p = 0.009$).

3.3. Inter-site differences in the degree of mineralization

In addition to the femoral diaphysis, we have analyzed the qBEI parameters in distal radius, iliac crest and lumbar vertebra between the treatment-naïve osteoporosis and bisphosphonate-treated groups (Table 1). Different skeletal sites significantly differed in mean calcium content and peak calcium content ($p < 0.001$) (Table 1). We found no significant differences between osteoporosis and bisphosphonate groups; however, mineralization of long bones seemed to have different tendencies following bisphosphonate-treatment when compared to spine and iliac crest (Table 1). There were significant differences in Ca width among various skeletal sites and bony compartments ($p < 0.001$), and the osteoporosis group showed significantly more heterogeneous mineralization distribution compared to bisphosphonate group ($p = 0.008$) (Table 1).

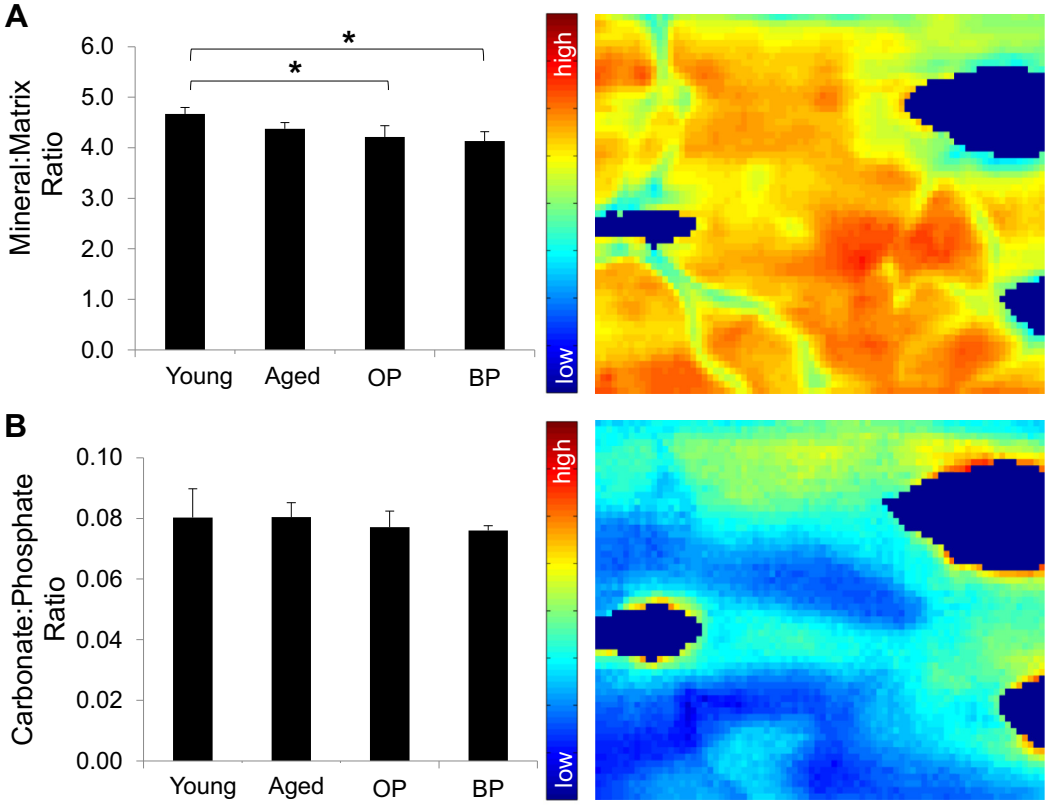

Fig. 3. Fourier transform infrared (FTIR) spectroscopy of the femoral cortical bone. The analyses refer to specimens from young, aged, untreated osteoporosis (OP) and bisphosphonate-treated (BP) women. Inter-group differences in mineral-to-matrix ratio (A) and carbonate-to-phosphate ratio (B). (* – $p < 0.05$). Error bars indicate SD.

Table 1
Inter-site differences in qBEI parameters: estimated marginal means (Repeated measures ANOVA).

Ca mean				Ca peak			Ca width			
Site	Group	Mean	SE	Inter-site	Mean	SE	Inter-site	Mean	SE	Inter-site
Vertebral	OPO	22.284	0.493	b	22.933	0.455	b	2.993	0.112	b
Trabeculae	BP	23.007	0.441		23.520	0.394		2.775	0.097	
Femur	OPO	23.963	0.237	a	24.533	0.259	a	2.645	0.045	a,d
cortex	BP	23.703	0.195		24.160	0.225		2.505	0.039	
Iliac crest	OPO	22.583	0.313	b	23.067	0.316	b	2.820	0.053	d
Cortex	BP	22.839	0.271		23.300	0.274		2.535	0.046	
Iliac crest	OPO	23.244	0.333	c	23.893	0.330	c	3.158	0.062	b,c
Trabeculae	BP	24.060	0.289		24.520	0.286		2.821	0.054	
Radius	OPO	24.838	0.449	a,c	25.600	0.475	a,c	2.789	0.084	a,d
Cortex	BP	24.495	0.389		25.100	0.411		2.648	0.073	
Radius	OPO	25.829	0.506	a,b,c	26.32	0.481	a,b,c	2.899	0.112	b,c
Trabeculae	BP	24.659	0.438		25.36	0.416		3.081	0.097	

a – Significantly different from vertebral trabeculae.
b – Significantly different from femoral cortex.
c – Significantly different from iliac cortex.
d – Significantly different from iliac trabeculae.

3.4. Haversian systems per bone area in the femoral cortex

The number of Haversian systems per bone area significantly depended on the study group ($p = 0.002$). Specifically, post-hoc tests revealed significantly higher values in the osteoporosis group (21.3 ± 0.7 Haversian canals per mm^2 bone area) when compared with the young (16.6 ± 1.0 Haversian canals/mm^2 – $p = 0.004$) and bisphosphonate-treated groups (17.7 ± 0.8 Haversian canals/mm^2 – $p = 0.013$), and a tendency to lower values in the young cases compared to the aged cases (20.0 ± 0.9 Haversian canals/mm^2 – $p = 0.084$).

3.5. Reference point indentation in the femoral cortex

Reference point indentation was used to characterize the mechanical properties of the bone specimens (Fig. 4A–E). The first cycle indentation distance (ID 1) and total indentation distance (TID) showed significant inter-group differences. Specifically, post-hoc tests revealed that young individuals had a lower ID 1 and TID than aged cases, individuals with untreated osteoporosis and bisphosphonate-treated individuals (Fig. 4B, C).

3.6. Relationship between matrix composition and indentation properties

The first cycle indentation distance (ID 1) and total indentation distance (TID) inversely correlated with the Ca mean value measured through qBEI on the femoral cortex ($r = -0.385$, $p = 0.039$; $r = -0.399$, $p = 0.032$; respectively). Additionally, the first cycle indentation distance (ID 1), total indentation distance (TID) and indentation distance increase (IDI) negatively correlated with the mineral-to-matrix ratio measured through FTIR ($r = -0.537$, $p = 0.003$; $r = -0.582$, $p = 0.001$; $r = -0.481$, $p = 0.01$; respectively).

3.7. Compartment-specific dependence of structure and mineralization indices

The obtained data on the bone structure and the mineralization shows that periosteal and endosteal cortical bone compartments differ from each other. The statistical evaluation of compartment-specificity can be found as Supplementary data.

4. Discussion

Osteoporosis is the most common bone disease in the world associated with bone loss, fractures and decreased quality of life [50]; a common treatment option is a class of drugs called bisphosphonates that act predominantly by suppressing bone resorption [26,51]. However, the effects of long-term bisphosphonate treatment on bone quality and the specific consequences for human cortical bone are understudied. Moreover, the characteristics of bone material immanent to several biological or medical conditions (i.e.: aging, disease and pharmacological treatment) require comprehensive analyses to elucidate variability in the bone structure and composition. Here, on a set of samples from young, aged, treatment-naïve osteoporotic and bisphosphonate-treated bone, we look for trends in cortical bone quality by investigating the microstructural morphology (*i.e.,* number of osteons and presence of total and hypermineralized osteocyte lacunae), the mineralization distribution, and the mechanical properties. Overall our goal was to document bone material variability in various conditions, and specifically to determine whether treatment with bisphosphonates has a beneficial effect on cortical bone.

Alendronate is a bisphosphonate best known for its targeted effect on osteoclast bone cells. During treatment, alendronate accumulates in bone tissue, binds to hydroxy-apatite and is ingested by osteoclasts [52,53]. In this way, alendronate reduces resorption of bone with initially limited effects on the deposition of bone (*i.e.,* osteoblast activity) [54]. In trabecular bone, bisphosphonates are particularly potent [53,55,56] because the large surface-area-to-volume ratio and higher metabolic activity facilitate their large-scale incorporation into the mineralized bone matrix. Thus, bisphosphonates generally increase bone mass in trabecular regions [57–59]. In addition, bisphosphonates binding affinity influences their distribution through bone compartments [53].

The effect of bisphosphonates on cortical bone has been studied much less [51,60]. In cortical bone, the surface-to-volume ratio is about five times lower than in cancellous bone [61], which may reduce the bisphosphonates' influence on cortical osteoclasts. Yet, here, we see significant changes in the microstructural morphology of the cortex between the young, aged, untreated osteoporotic, and bisphosphonate-treated osteoporotic individuals. One feature that stands out is the differential occurrence of mineralized lacunae (micropetrosis). While the exact mechanism of lacunar mineralization is not yet clear, it is known that osteocytes die with aging

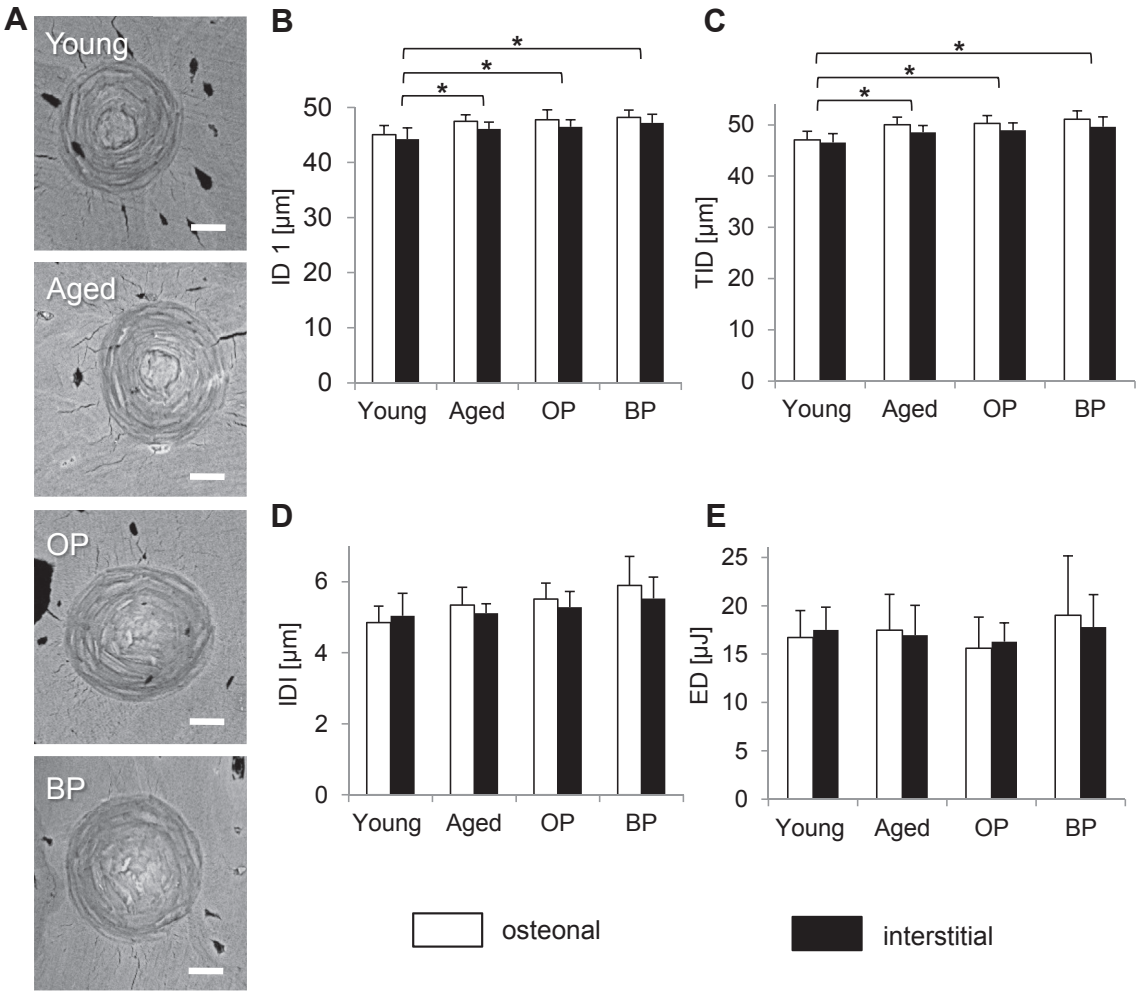

Fig. 4. Reference Point Indentation of the femoral cortical bone. The analyses refer to specimens from young, aged, untreated osteoporosis (OP) and bisphosphonate-treated (BP) women. (A) Representative backscattered electron images showing the indents made by RPI (Scale bar 20 µm). (B) Inter-group differences in first cycle indentation distance – ID 1, (C) total indentation distance – TID, (D) indentation distance increase – IDI, and (E) average dissipated energy – ED. (* – $p < 0.05$). Error bars indicate SD. Note that white columns show osteonal whereas black columns represent interstitial bone properties (ID 1 and TID are significantly higher in osteonal than interstitial cortical bone, $p < 0.05$ – ANOVA for repeated measurements).

[62,63] and mineralized lacunae appear mostly in aged tissue [12,19,62]. However, not only do the aged cases have a higher number of mineralized lacunae than young cases, but our findings show that osteoporosis is associated with even more frequent mineralized lacunar occlusions. Nevertheless, after long-term alendronate treatment, the amount of mineralized lacunae significantly drops.

The lower amount of mineralized lacunae in bisphosphonate-treated osteoporotic cases supports recent studies that have found bisphosphonates to have a beneficial effect on osteocytes' and osteoblasts' viability [32,33]. In particular, due to the lower surface-to-volume ratio in cortical bone, bisphosphonates cannot have as large of an impact on remodeling by controlling osteoclastic resorption as they do in trabecular bone. However, (depending on their affinity) at the low concentrations found in cortical bone [55,64] bisphosphonates have been shown to increase the vitality of osteoblasts and osteocytes [65]. Thus, our findings indicate that exposure to low levels of alendronate in cortical bone may keep osteocytes alive by preventing cell death and the subsequent formation of mineralized lacunae.

The beneficial effects of bisphosphonates on osteocytes in cortical bone are also supported by our observations of the osteon density. In comparison to young cases, an increase in the amount of osteons was found in the femoral cortex of the aged and osteoporotic groups, which is consistent with previous studies [66]. The higher number of osteons in aged and osteoporotic cases most likely occurs due to imbalances in bone turnover causing higher amounts of bone resorption. Indeed, in aged and osteoporotic cases, previous studies have found smaller osteon diameters indicating altered osteoclast resorption and smaller wall thicknesses indicating altered osteoblastic deposition of mineralized bone [65]. Contrary to findings in ribs of adult beagle dogs [34], after bisphosphonate treatment, we have observed a decrease in number of osteons and increase in their size [67] in the femoral cortex, which may be perceived as “restoration” to osteon characteristics in young individuals. Interestingly, the reduced number of osteons in bisphosphonate-treated cortical bone is most likely not a pure result of the bisphosphonates' ability to regulate osteoclastic resorption as in trabecular bone, because the cortex's low surface-to-volume ratio leads to lower concentrations of bisphosphonates within complete cortex [53]. In fact, the size and number of osteons might be rebalanced in the cortex after bisphosphonate treatment due to persistent presence of osteoclasts that may stabilize bone turnover on a lower level without complete uncoupling of bone

remodeling cells [56] and due to the beneficial effects of the low levels of bisphosphonates on the osteocytes and osteoblasts. Indeed, we have shown that after bisphosphonate treatment there are fewer mineralized lacunae. The mineralization of lacunae has implications for bone matrix quality because partial or full occlusion of the lacunae would decrease the cell's ability to sense and transduce normal skeletal loading through fluid flow and consequently hamper bone's adaptive response [20,68]. Clearly, if the vitality of the osteocytes is stimulated [31,33] and the communication between cells is maintained [2], remodeling will progress much more effectively than after widespread micropetrosis, i.e., cell death and mineralization of lacunae. Therefore, the beneficial effects of low levels of bisphosphonates on the osteocytes in cortical bone appear to preserve the osteocytes' vitality, maintain communication between cells, prevent the accumulation of mineralized lacunae, and foster normal remodeling to produce a size and number of osteons similar to young bone. As osteocytes are major orchestrators of bone remodeling and as such contribute to tissue age and matrix quality, their impact on human bone should be discussed as an important aspect when designing the next generation of bio-inspired, bio-active materials for bone replacement. Specifically, the absence or damage to the osteocyte-lacunar system in bone grafts may be a major contributor to the adverse effects on bone regeneration [69,70], failures and reduced biomechanical properties during the application of graft material.

In terms of the mineralization of the femoral cortical compartment, we observed a steadily decreasing degree of mineralization from young to treatment-naïve and bisphosphonate-treated cases. The lower bone mineralization in osteoporotic tissue compared to healthy age-matched controls supports some previous qBEI results [71] and may be due to the changed bone remodeling activity, which would create more undermineralized bone packets with a lower mineral content in cortical bone. However, caution is necessary as the reports on increased mineralization levels in fragility fracture patients are frequent and the complex trends may depend on the skeletal site, compartment or population [39,47,72]. Here the observed trend in mineralization of the cortical bone does vary from some trends previously published for trabecular regions and/or other skeletal sites; however, inter-site and bone compartment differences in the mineralization pattern seem to be a characteristic feature in the human skeleton which may be even enhanced by bisphosphonate treatment. Even in normal conditions, subtrochanteric and iliac bone differ in terms of mineralization level [73]. We found that after bisphosphonate treatment only the vertebral and iliac crest trabecular bone showed a tendency towards an increased bone mineralization distribution, which supports previous studies [51,60,74–77]. Conversely, in the femur and radius, the bisphosphonate treatment was even associated with a tendency to lower mineralization distribution, which is in line with previously observed inter-site differences in densitometric and histomorphometric properties [78–80]. As the femur, radius, vertebrae and iliac crest are subject to differential remodeling rates [81,82], it is possible that the effect of the bisphosphonates may depend on the pre-treatment remodeling rates, perfusion and metabolism in these skeletal sites [53,78,83] as well as different structure and load patterns [84]. Moreover, our results showed that trabecular bone sites show more differences in mineralization between untreated and bisphosphonate-treated osteoporotic cases than the cortical sites (Table 1), which is compatible with previous hypotheses about different dose–response behaviors of cancellous vs. cortical compartments, due to higher bisphosphonates incorporation in trabeculae [78]. Moreover, the degree of alendronate's affinity for bone matrix and its depth of penetration would influence differential distribution between the compartments [53].

In regard to mechanical properties, it is, however, likely that both too low and too high mineralization patterns may render bone fragile [39,47,71] by reducing strength or work-to-fracture, respectively, as shown on vertebral bone [85]. Here, our reference point indentation measurements showed that the indentation distances of the aged, untreated osteoporotic and bisphosphonate-treated osteoporotic cases were all higher than of the young bone. The indentation distances correlated inversely with the mineralization level, supporting the previous observations that the resistance to indentation (*i.e.,* hardness) of a material depends on its mineral content [49,86,87]. However, the osteon distribution could be another indicator of fracture toughness. Higher densities of osteons generally have lower toughness, whereas lower densities have higher toughness. The low density cases have a single crack deflection, whereas the high density has many small deflections, which ends up looking like a large, straight crack [88,89].

5. Conclusions

Here, we investigate changes in bone quality in cortical bone from the femoral diaphysis and show that multiple structural and compositional changes of bone material reflect differential biological/mechanical characteristics in aging, osteoporosis and alendronate-treatment states. In particular, bisphosphonates have a strong effect on this cortical site even though many of the trends are contradictory to the known effects of bisphosphonates on trabecular bone. An important aspect of bisphosphonate-treatment in cortical bone is the renewed quality of the osteocytes (*i.e.,* fewer mineralized osteocyte lacunae) and perhaps the ability to restore normal bone remodeling (*i.e.,* fewer and larger osteons). Our specific conclusions are the following:

1. Significantly higher amounts of mineralized osteocyte lacunae were found in the femoral cortex with aging and osteoporosis, which is attributed to increased osteocyte apoptosis.
2. Bisphosphonates may improve the vitality of cortical bone osteocytes, resulting in less cellular apoptosis as observed through the lower amount of mineralized lacunae, which has an important effect on bone mechanical integrity.
3. Additionally, the improved vitality of the osteocytes and osteoblasts in the femoral cortex due to bisphosphonate treatment as well as the lower amount of mineralized lacunae creates an environment that promotes cellular communication and normal remodeling conditions. Thus, the amount of osteons and their size in bisphosphonate-treated cases may be more characteristic of young bone.
4. The mineral distribution in the femoral osteoporotic cortical bone was lower in comparison to young cases, which may reflect increased surface area undergoing remodeling and insufficient secondary mineralization associated with osteoporosis.
5. The indentation distances measured via reference point indentation on the femoral cortices indicate that the young cases have the highest resistance to deformation. These results follow the overall trends in the degree of mineralization measured via quantitative backscattered electron imaging and FTIR.
6. Bisphosphonates clearly have varying effects on different skeletal sites, which may be partly the result of the surface-to-volume ratio of the tissue. Here, quantitative backscattered electron imaging of the bone mineral density distribution indicates that trabecular regions, specifically in the iliac crest and lumbar vertebra, tend to have a higher mineralization after bisphosphonate treatment, while the primarily cortical regions, specifically the distal radius and femoral diaphysis, have slightly decreased mineralization level.

7. The hierarchical analysis of bone material with different biological and mechanical characteristics (healthy bone, bone altered by aging, bone affected by disease, and pharmacologically altered bone) reveals its strengths and weaknesses that should be considered when designing new microstructures and compositions for bone replacement materials.

Acknowledgments

This work was supported by the Emmy Noether program BU 2562/2-1 of the 'Deutsche Forschungsgemeinschaft' (DFG, German Research Foundation), Southeast-Europe Cooperation of the University Medical Center Hamburg-Eppendorf, Deutscher Akademischer Austauschdienst grant no. A/11/83161 (DAAD, German Academic Exchange Service) and Serbian Ministry of Education and Science grant no. III45005.

Appendix A. Supplementary data

Supplementary data related to this article can be found at http://dx.doi.org/10.1016/j.biomaterials.2014.12.015.

References

[1] Zimmermann EA, Gludovatz B, Schaible E, Busse B, Ritchie RO. Fracture resistance of human cortical bone across multiple length-scales at physiological strain rates. Biomaterials 2014;35(21):5472–81.
[2] Milovanovic P, Zimmermann EA, Hahn M, Djonic D, Püschel K, Djuric M, et al. Osteocytic canalicular networks: morphological implications for altered Mechanosensitivity. ACS Nano 2013;7(9):7542–51.
[3] Klein-Nulend J, van der Plas A, Semeins C, Ajubi N, Frangos J, Nijweide P, et al. Sensitivity of osteocytes to biomechanical stress in vitro. FASEB J 1995;9(5):441–5.
[4] Adachi T, Aonuma Y, Tanaka M, Hojo M, Takano-Yamamoto T, Kamioka H. Calcium response in single osteocytes to locally applied mechanical stimulus: differences in cell process and cell body. J Biomech 2009;42(12):1989–95.
[5] McGarry JG, Klein-Nulend J, Mullender MG, Prendergast PJ. A comparison of strain and fluid shear stress in stimulating bone cell responses – a computational and experimental study. FASEB J 2005;19(3):482–4.
[6] Vatsa A, Mizuno D, Smit TH, Schmidt CF, MacKintosh FC, Klein-Nulend J. Bio imaging of intracellular NO production in single bone cells after mechanical stimulation. J Bone Miner Res 2006;21(11):1722–8.
[7] Vatsa A, Smit TH, Klein-Nulend J. Extracellular NO signalling from a mechanically stimulated osteocyte. J Biomech 2007;40:S89–95.
[8] You L-D, Weinbaum S, Cowin SC, Schaffler MB. Ultrastructure of the osteocyte process and its pericellular matrix. Anat Rec A 2004;278A(2):505–13.
[9] Sauren YM, Mieremet RH, Groot CG, Scherft JP. An electron microscopic study on the presence of proteoglycans in the mineralized matrix of rat and human compact lamellar bone. Anat Rec 1992;232(1):36–44.
[10] Lane NE, Yao W, Balooch M, Nalla RK, Balooch G, Habelitz S, et al. Glucocorticoid-treated mice have localized changes in trabecular bone material properties and osteocyte lacunar size that are not observed in placebo-treated or estrogen-deficient mice. J Bone Miner Res 2006;21(3):466–76.
[11] Zhang K, Barragan-Adjemian C, Ye L, Kotha S, Dallas M, Lu Y, et al. E11/gp38 selective expression in osteocytes: regulation by mechanical strain and role in dendrite elongation. Mol Cell Biol 2006;26(12):4539–52.
[12] Busse B, Djonic D, Milovanovic P, Hahn M, Püschel K, Ritchie RO, et al. Decrease in the osteocyte lacunar density accompanied by hypermineralized lacunar occlusion reveals failure and delay of remodeling in aged human bone. Aging Cell 2010;9(6):1065–75.
[13] Bell LS, Kayser M, Jones C. The mineralized osteocyte: a living fossil. Am J Phys Anthropol 2008;137(4):449–56.
[14] Qiu S, Sudhaker Rao D, Fyhrie DP, Palnitkar S, Parfitt AM. The morphological association between microcracks and osteocyte lacunae in human cortical bone. Bone 2005;37(1):10–5.
[15] Vashishth D, Verborgt O, Divine G, Schaffler MB, Fyhrie DP. Decline in osteocyte lacunar density in human cortical bone is associated with accumulation of microcracks with age. Bone 2000;26(4):375–80.
[16] Burger EH, Klein-Nulend J. Mechanotransduction in bone – role of the lacuno-canalicular network. FASEB J 1999;13(9001):101–12.
[17] van Hove RP, Nolte PA, Vatsa A, Semeins CM, Salmon PL, Smit TH, et al. Osteocyte morphology in human tibiae of different bone pathologies with different bone mineral density – is there a role for mechanosensing? Bone 2009;45(2):321–9.
[18] Vatsa A, Breuls RG, Semeins CM, Salmon PL, Smit TH, Klein-Nulend J. Osteocyte morphology in fibula and calvaria — is there a role for mechanosensing? Bone 2008;43(3):452–8.
[19] Frost HM. Micropetrosis. J Bone Jt Surg Am 1960;42:144–50.
[20] Carpentier VT, Wong J, Yeap Y, Gan C, Sutton-Smith P, Badiei A, et al. Increased proportion of hypermineralized osteocyte lacunae in osteoporotic and osteoarthritic human trabecular bone: implications for bone remodeling. Bone 2012;50(3):688–94.
[21] Bouxsein M. Bone quality: where do we go from here? Osteoporos Int 2003;14(5):118–27.
[22] Ritchie RO. The conflicts between strength and toughness. Nat Mater 2011;10(11):817–22.
[23] Busse B, Bale HA, Zimmermann EA, Panganiban B, Barth HD, Carriero A, et al. Vitamin d deficiency induces early signs of aging in human bone, increasing the risk of fracture. Sci Transl Med 2013;5(193):193ra188.
[24] Kingsmill VJ, Boyde A. Mineralisation density of human mandibular bone: quantitative backscattered electron image analysis. J Anat 1998;192(2):245–56.
[25] Black DM, Schwartz AV, Ensrud K, Cauley J, Levis S, Quandt SA, et al. Effects of continuing or stopping alendronate after 5 years of treatment: the fracture intervention trial long-term extension (flex): a randomized trial. J Am Med Assoc 2006;296(24):2927–38.
[26] Russell RG. Bisphosphonates: the first 40 years. Bone 2011;49(1):2–19.
[27] Bone HG, Hosking D, Devogelaer J-P, Tucci JR, Emkey RD, Tonino RP, et al. Ten years' experience with alendronate for osteoporosis in postmenopausal women. N Engl J Med 2004;350(12):1189–99.
[28] Cummings SR, Black DM, Thompson DE, et al. Effect of alendronate on risk of fracture in women with low bone density but without vertebral fractures: results from the fracture intervention trial. J Am Med Assoc 1998;280(24):2077–82.
[29] Shane E, Burr D, Abrahamsen B, Adler RA, Brown TD, Cheung AM, et al. Atypical subtrochanteric and diaphyseal femoral fractures: second report of a task force of the American Society for Bone and Mineral Research. J Bone Miner Res 2014;29(1):1–23.
[30] Shane E, Burr D, Ebeling PR, Abrahamsen B, Adler RA, Brown TD, et al. Atypical subtrochanteric and diaphyseal femoral fractures: report of a task force of the American Society for Bone and Mineral Research. J Bone Miner Res 2010;25(11):2267–94.
[31] Brennan O, Kennedy OD, Lee TC, Rackard SM, O'Brien FJ. Effects of estrogen deficiency and bisphosphonate therapy on osteocyte viability and microdamage accumulation in an ovine model of osteoporosis. J Orthop Res 2011;29(3):419–24.
[32] Bellido T, Plotkin LI. Novel actions of bisphosphonates in bone: preservation of osteoblast and osteocyte viability. Bone 2011;49(1):50–5.
[33] Plotkin LI, Weinstein RS, Parfitt AM, Roberson PK, Manolagas SC, Bellido T. Prevention of osteocyte and osteoblast apoptosis by bisphosphonates and calcitonin. J Clin Invest 1999;104(10):1363–74.
[34] Bajaj D, Geissler JR, Allen MR, Burr DB, Fritton JC. The resistance of cortical bone tissue to failure under cyclic loading is reduced with alendronate. Bone 2014;64(0):57–64.
[35] Hahn M, Vogel M, Delling G. Undecalcified preparation of bone tissue: report of technical experience and development of new methods. Virchows Arch A Pathol Anat Histopathol 1991;418(1):1–7.
[36] Donath K, Breuner G. A method for the study of undecalcified bones and teeth with attached soft tissues. The Säge-Schliff (sawing and grinding) technique. J Oral Pathol 1982;11(4):318–26.
[37] Doube M, Kłosowski MM, Arganda-Carreras I, Cordelières FP, Dougherty RP, Jackson JS, et al. BoneJ: free and extensible bone image analysis in ImageJ. Bone 2010;47(6):1076–9.
[38] Busse B, Hahn M, Schinke T, Püschel K, Duda GN, Amling M. Reorganization of the femoral cortex due to age-, sex-, and endoprosthetic-related effects emphasized by osteonal dimensions and remodeling. J Biomed Mater Res A 2010;92A(4):1440–51.
[39] Busse B, Hahn M, Soltau M, Zustin J, Püschel K, Duda GN, et al. Increased calcium content and inhomogeneity of mineralization render bone toughness in osteoporosis: mineralization, morphology and biomechanics of human single trabeculae. Bone 2009;45(6):1034–43.
[40] Regelsberger J, Milovanovic P, Schmidt T, Hahn M, Zimmermann E, Tsokos M, et al. Changes to the cell, tissue and architecture levels in cranial suture synostosis reveal a problem of timing in bone development. Eur Cell Mater 2012;24:441–58.
[41] Roschger P, Fratzl P, Eschberger J, Klaushofer K. Validation of quantitative backscattered electron imaging for the measurement of mineral density distribution in human bone biopsies. Bone 1998;23(4):319–26.
[42] Roschger P, Paschalis EP, Fratzl P, Klaushofer K. Bone mineralization density distribution in health and disease. Bone 2008;42(3):456–66.
[43] Koehne T, Marshall RP, Jeschke A, Kahl-Nieke B, Schinke T, Amling M. Osteopetrosis, osteopetrorickets and hypophosphatemic rickets differentially affect dentin and enamel mineralization. Bone 2013;53(1):25–33.
[44] Hansma P, Turner P, Drake B, Yurtsev E, Proctor A, Mathews P, et al. The bone diagnostic instrument II: indentation distance increase. Rev Sci Instrum 2008;79(6):064303–8.
[45] Güerri-Fernández RC, Nogués X, Quesada Gómez JM, Torres del Pliego E, Puig L, García-Giralt N, et al. Microindentation for in vivo measurement of bone tissue material properties in atypical femoral fracture patients and controls. J Bone Miner Res 2013;28(1):162–8.
[46] Diez-Perez A, Güerri R, Nogues X, Cáceres E, Peña MJ, Mellibovsky L, et al. Microindentation for in vivo measurement of bone tissue mechanical properties in humans. J Bone Miner Res 2010;25(8):1877–85.

[47] Milovanovic P, Rakocevic Z, Djonic D, Zivkovic V, Hahn M, Nikolic S, et al. Nano-structural, compositional and micro-architectural signs of cortical bone fragility at the superolateral femoral neck in elderly hip fracture patients vs. healthy aged controls. Exp Gerontol 2014;55:19–28.
[48] Gallant MA, Brown DM, Organ JM, Allen MR, Burr DB. Reference-point indentation correlates with bone toughness assessed using whole-bone traditional mechanical testing. Bone 2013;53(1):301–5.
[49] Thurner PJ, Erickson B, Turner P, Jungmann R, Lelujian J, Proctor A, et al. The effect of NaF in vitro on the mechanical and material properties of trabecular and cortical bone. Adv Mater 2009;21(4):451–7.
[50] Cole Z, Dennison E, Cooper C. Osteoporosis epidemiology update. Curr Rheumatol Rep 2008;10(2):92–6.
[51] Bala Y, Farlay D, Chapurlat RD, Boivin G. Modifications of bone material properties in postmenopausal osteoporotic women long-term treated with alendronate. Eur J Endocrinol 2011;165(4):647–55.
[52] Busse B, Jobke B, Hahn M, Priemel M, Niecke M, Seitz S, et al. Effects of strontium ranelate administration on bisphosphonate-altered hydroxyapatite: matrix incorporation of strontium is accompanied by changes in mineralization and microstructure. Acta Biomater 2010;6(12):4513–21.
[53] Turek J, Ebetino FH, Lundy M, Sun S, Kashemirov B, McKenna C, et al. Bisphosphonate binding affinity affects drug distribution in both intracortical and trabecular bone of rabbits. Calcif Tissue Int 2012;90(3):202–10.
[54] Ott SM. What is the optimal duration of bisphosphonate therapy? Cleve Clin J Med 2011;78(9):619–30.
[55] Pazianas M, van der Geest S, Miller P. Bisphosphonates and bone quality. BoneKEy Rep 2014;3(529):1–8.
[56] Jobke B, Milovanovic P, Amling M, Busse B. Bisphosphonate-osteoclasts: changes in osteoclast morphology and function induced by antiresorptive nitrogen-containing bisphosphonate treatment in osteoporosis patients. Bone 2014;59(0):37–43.
[57] Chavassieux PM, Arlot ME, Reda C, Wei L, Yates AJ, Meunier PJ. Histomorphometric assessment of the long-term effects of alendronate on bone quality and remodeling in patients with osteoporosis. J Clin Invest 1997;100(6):1475–80.
[58] Recker R, Masarachia P, Santora A, Howard T, Chavassieux P, Arlot M, et al. Trabecular bone microarchitecture after alendronate treatment of osteoporotic women. Curr Med Res Opin 2005;21(2):185–94.
[59] Diab T, Wang J, Reinwald S, Guldberg RE, Burr DB. Effects of the combination treatment of raloxifene and alendronate on the biomechanical properties of vertebral bone. J Bone Miner Res 2011;26(2):270–6.
[60] Bala Y, Depalle B, Farlay D, Douillard T, Meille S, Follet H, et al. Bone micromechanical properties are compromised during long-term alendronate therapy independently of mineralization. J Bone Miner Res 2012;27(4):825–34.
[61] Parfitt AM. Skeletal heterogeneity and the purposes of bone remodeling: implications for the understanding of osteoporosis. In: Marcus R, Feldman D, Dempster DW, Luckey M, Cauley JA, editors. Osteoporosis. ed. San Diego: Academic Press; 2013. p. 855–72.
[62] Frost HM. Vivo osteocyte death. J Bone Jt Surg Am 1960;42(1):138–43.
[63] Noble BS, Reeve J. Osteocyte function, osteocyte death and bone fracture resistance. Mol Cell Endocrinol 2000;159(1–2):7–13.
[64] Zebaze RM, Libanati C, Austin M, Ghasem-Zadeh A, Hanley DA, Zanchetta JR, et al. Differing effects of denosumab and alendronate on cortical and trabecular bone. Bone 2014;59(0):173–9.
[65] Plotkin LI, Lezcano V, Thostenson J, Weinstein RS, Manolagas SC, Bellido T. Connexin 43 is required for the anti-apoptotic effect of bisphosphonates on osteocytes and osteoblasts in vivo. J Bone Min Res 2008;23(11):1712–21.
[66] Zimmermann EA, Schaible E, Bale H, Barth HD, Tang SY, Reichert P, et al. Age-related changes in the plasticity and toughness of human cortical bone at multiple length scales. Proc Natl Acad Sci U S A 2011;108(35):14416–21.
[67] Bernhard A, Milovanovic P, Zimmermann EA, Hahn M, Djonic D, Krause M, et al. Micro-morphological properties of osteons reveal changes in cortical bone stability during aging, osteoporosis, and bisphosphonate treatment in women. Osteoporos Int 2013;24(10):2671–80.
[68] Bonivtch AR, Bonewald LF, Nicolella DP. Tissue strain amplification at the osteocyte lacuna: a microstructural finite element analysis. J Biomech 2007;40(10):2199–206.
[69] Sun Y-X, Sun C-L, Tian Y, Xu W-X, Zhou C-L, Xi C-Y, et al. A comparison of osteocyte bioactivity in fine particulate bone powder grafts vs larger bone grafts in a rat bone repair model. Acta Histochem 2014;116(6):1015–21.
[70] Miron RJ, Gruber R, Hedbom E, Saulacic N, Zhang Y, Sculean A, et al. Impact of bone harvesting techniques on cell viability and the release of growth factors of autografts. Clin Implant Dent Relat Res 2013;15(4):481–9.
[71] Fratzl-Zelman N, Roschger P, Gourrier A, Weber M, Misof B, Loveridge N, et al. Combination of nanoindentation and quantitative backscattered electron imaging revealed altered bone material properties associated with femoral neck fragility. Calcif Tissue Int 2009;85(4):335–43.
[72] Wu Y, Bergot C, Jolivet E, Zhou LQ, Laredo J-D, Bousson V. Cortical bone mineralization differences between hip-fractured females and controls. A microradiographic study. Bone 2009;45(2):207–12.
[73] Donnelly E, Meredith DS, Nguyen JT, Boskey AL. Bone tissue composition varies across anatomic sites in the proximal femur and the iliac crest. J Orthop Res 2012;30(5):700–6.
[74] Roschger P, Rinnerthaler S, Yates J, Rodan GA, Fratzl P, Klaushofer K. Alendronate increases degree and uniformity of mineralization in cancellous bone and decreases the porosity in cortical bone of osteoporotic women. Bone 2001;29(2):185–91.
[75] Roschger P, Lombardi A, Misof BM, Maier G, Fratzl-Zelman N, Fratzl P, et al. Mineralization density distribution of postmenopausal osteoporotic bone is restored to normal after long-term alendronate treatment: qBEI and sSAXS data from the fracture intervention trial long-term extension (FLEX). J Bone Miner Res 2010;25(1):48–55.
[76] Borah B, Dufresne TE, Ritman EL, Jorgensen SM, Liu S, Chmielewski PA, et al. Long-term risedronate treatment normalizes mineralization and continues to preserve trabecular architecture: sequential triple biopsy studies with micro-computed tomography. Bone 2006;39(2):345–52.
[77] Krause M, Soltau M, Zimmermann E, Hahn M, Kornet J, Hapfelmeier A, et al. Effects of long-term alendronate treatment on bone mineralisation, resorption parameters and biomechanics of single human vertebral trabeculae. Eur Cell Mater 2014;28:152–65.
[78] Smith SY, Recker RR, Hannan M, Müller R, Bauss F. Intermittent intravenous administration of the bisphosphonate ibandronate prevents bone loss and maintains bone strength and quality in ovariectomized cynomolgus monkeys. Bone 2003;32(1):45–55.
[79] Hu JH, Ding M, Søballe K, Bechtold JE, Danielsen CC, Day JS, et al. Effects of short-term alendronate treatment on the three-dimensional microstructural, physical, and mechanical properties of dog trabecular bone. Bone 2002;31(5):591–7.
[80] Allen MR, Kubek DJ, Burr DB. Cancer treatment dosing regimens of zoledronic acid result in near-complete suppression of mandible intracortical bone remodeling in beagle dogs. J Bone Miner Res 2010;25(1):98–105.
[81] Eventov I, Frisch B, Cohen Z, Hammel I. Osteopenia, hematopoiesis, and bone remodelling in iliac crest and femoral biopsies: a prospective study of 102 cases of femoral neck fractures. Bone 1991;12(1):1–6.
[82] Schnitzler CM, Biddulph SL, Mesquita JM, Gear KA. Bone structure and turnover in the distal radius and iliac crest: a histomorphometric study. J Bone Miner Res 1996;11(11):1761–8.
[83] Lin JH. Bisphosphonates: a review of their pharmacokinetic properties. Bone 1996;18(2):75–85.
[84] Burghardt AJ, Kazakia GJ, Sode M, de Papp AE, Link TM, Majumdar S. A longitudinal HR-pQCT study of alendronate treatment in postmenopausal women with low bone density: relations among density, cortical and trabecular microarchitecture, biomechanics, and bone turnover. J Bone Miner Res 2010;25(12):2558–71.
[85] Ciarelli TE, Fyhrie DP, Parfitt AM. Effects of vertebral bone fragility and bone formation rate on the mineralization levels of cancellous bone from white females. Bone 2003;32(3):311–5.
[86] Currey JD. Bones: structure and mechanics. Princeton, N. J.: Princeton University Press; 2002.
[87] Bala Y, Depalle B, Douillard T, Meille S, Clément P, Follet H, et al. Respective roles of organic and mineral components of human cortical bone matrix in micromechanical behavior: an instrumented indentation study. J Mech Behav Biomed Mater 2011;4(7):1473–82.
[88] Koester KJ, Barth HD, Ritchie RO. Effect of aging on the transverse toughness of human cortical bone: evaluation by R-curves. J Mech Behav Biomed Mater 2011;4(7):1504–13.
[89] Nalla RK, Kruzic JJ, Kinney JH, Balooch M, Ager Iii JW, Ritchie RO. Role of microstructure in the aging-related deterioration of the toughness of human cortical bone. Mater Sci Eng C 2006;26(8):1251–60.